PHYSICAL REVIEW A VOLUME 16, NUMBER 3 SEPTEMBER 1977

Electron impact excitation of the electronic states of N_2. III. Transitions in the 12.5–14.2-eV energy-loss region at incident energies of 40 and 60 eV‡

A. Chutjian
Jet Propulsion Laboratory, California Institute of Technology, Pasadena, California 91103

D. C. Cartwright
Theoretical Division, Los Alamos Scientific Laboratory, University of California, Los Alamos, New Mexico 87545

S. Trajmar
Jet Propulsion Laboratory, California Institute of Technology, Pasadena, California 91103

(Received 11 May 1977)

Normalized absolute differential and integral cross sections for electron-impact excitation of five optically-allowed singlet states, two known triplet states, and two unknown triplet-like states of N_2, lying in the energy-loss range 12.5–14.2 eV, have been determined by analysis of electron energy-loss data at incident electron energies of 40 and 60 eV. The range of scattering angles considered in this work was 5° to 138°. The optically allowed transitions are to the $b\,^1\Pi_u$, $c\,^1\Pi_u$, $c'\,^1\Sigma_u^+$, $o\,^1\Pi_u$, and $b'\,^1\Sigma_u^+$ states and the known triplet excitations are to the $F\,^3\Pi_u$ and $G\,^3\Pi_u$ states. Cross sections for excitation to two unidentified triplet-like states at 13.155 and 13.395 eV were also obtained from the data analysis. The relationship of the generalized oscillator strength for the dipole-allowed states obtained from the present measurements to known optical oscillator strengths is discussed.

I. INTRODUCTION

Knowledge of differential and integral cross sections for the excitation of electronic transitions of N_2 by intermediate-energy electrons is needed in modeling various environments in which N_2 is a significant component. These include the N_2 laser,[1] Earth's upper atmosphere[2] (including auroral regions), and the Martian atmosphere.[3] Considering the importance of N_2 in these different plasmas, it is somewhat surprising that no reliable or consistent set of absolute cross sections had been obtained for e-N_2 inelastic interactions in the very important intermediate energy region from a few eV above threshold to about 100 eV. In the preceding two papers we have reported differential[4] and integral[5] cross sections for excitation of the N_2 electronic states lying below 12.5 eV. In this third paper we report differential and integral cross sections for excitation of states in the 12.5–14.2 eV energy-loss range. It is in this energy-loss range that the lowest dipole-allowed transitions in N_2 are found.

A number of earlier electron-scattering studies have been carried out on electronic transitions lying in the 12–14 eV energy-loss range. Excitation of N_2 by energetic electrons (energies $\geq$25 keV) with detection of nearly forward-scattered electrons at moderate-to-high resolution[6,7] has yielded important spectroscopic information on transitions in this energy-loss range. At lower incident energies (E_0 = 48, 200, and 500 eV[8–11] and for small-angle scattering ($\theta < 13°$) relative intensities in the $b\,^1\Pi_u \leftarrow X\,^1\Sigma_g^+$ transition have been measured[8–10] and compared to optical intensities. Normalized absolute generalized oscillator strengths (GOS) have also been obtained.[11] These GOS represent integrals over several overlapping transitions under low-resolution (~0.6 eV) conditions. In other studies, relative intensities of bands in the $b \leftarrow X$ and the combined $c'\,^1\Sigma_u^+$, $c\,^1\Pi_u \leftarrow X$ transitions have been reported out to $\theta = 40°$ at E_0 of 15, 19.2, and 35 eV.[12,13] Measurements of e-N_2 scattering very close to threshold[14] (residual energies of 0.02 eV or less) at angles between 40° and 120° have provided important spectroscopic information on both optically allowed and forbidden transitions in the region 11.8–13.8 eV.

While the spectroscopy of this region is now fairly well understood and certain anomalies in the electron scattering versus optical absorption spectrum clarified,[15] no absolute electron scattering cross sections have previously been reported for these features. In the present paper we report normalized absolute differential cross sections (DCS's) for the five optically allowed transitions to the $b\,^1\Pi_u$, $b'\,^1\Sigma_u^+$, $c\,^1\Pi_u$, $c'\,^1\Sigma_u^+$, and $o\,^1\Pi_u$ states. Differential cross sections have also been measured to two known triplet states ($F\,^3\Pi_u$ and $G\,^3\Pi_u$) and to two unknown states (indicated here as $M1$ and $M2$).

In Sec. II we review briefly some of the details of the experimental and computer-unfolding methods used, including the method of normalization of the data to the absolute cross section scale. Results are given in Sec. III, and discussed and compared to results of other workers in Sec. IV.

II. EXPERIMENTAL AND COMPUTATIONAL METHODS

The electron scattering spectrometer used in the present measurements,[16] and a description of the data-analysis (computer unfolding) methods have been given earlier.[4, 5, 17] Details of the electron optics, and the use of zoom lenses to provide reliable inelastic-to-elastic scattering intensity ratios may be found in Ref. 18.

The electron-scattering apparatus uses a crossed electron-beam–N_2-beam geometry. The electron beam is defined in energy and angular spread by a hemispherical electron monochromator, and by the use of tube lenses with suitable defining apertures.[18] The incident current is typically 1–5 nA with a resolution of 0.045–0.065 eV (FWHM). Electrons scattered into a small solid angle (~1 $\times 10^{-3}$ sr) are focused, energy-analyzed, and detected with a spiral electron multiplier. Incident energies used in this study were 40 and 60 eV. The N_2 beam effused from a stainless-steel multichannel array having an aspect ratio of 100. Conventional amplification and multichannel pulse-counting techniques were used to record the energy-loss spectra. A step size of 0.002 eV was used, and recording times were typically 1–24 h, depending on the scattering angle and incident energy.

In each energy-loss spectrum, the analyzer first swept through the elastic scattering peak (energy loss $\Delta E = 0$ eV), then "jumped" to the region 12.5–14.2 eV of the desired inelastic features. Analyzer focusing voltages were set empirically so that focusing was optimal for both the elastic and inelastic features. These empirical voltages were very close to calculated ones for the analyzer optics.[18] This procedure ensured that reliable inelastic-to-elastic scattering ratios would be obtained.

The computational techniques used to unfold the electron energy-loss data have been described in detail in paper I and the application of the method to these energy-loss spectra differed only in the following detail. Strong perturbation among pairs

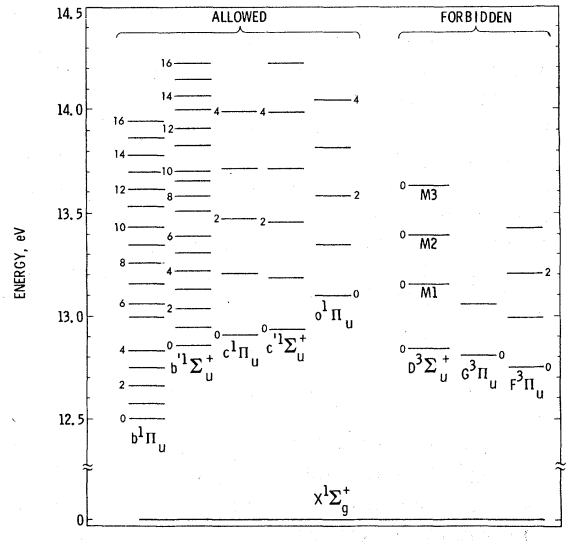

FIG. 1. Energy-level diagram for the vibrational levels in the optically allowed singlet and forbidden triplet electronic states of N_2, in the 12.5–14.3 eV energy region.

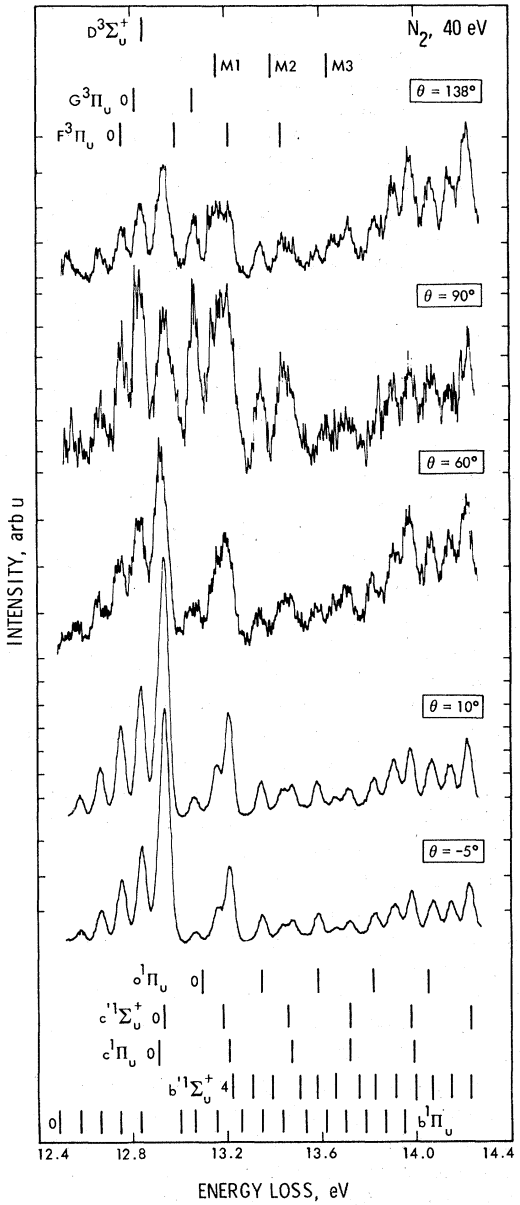

FIG. 2. Composite raw energy-loss spectra at 40 eV incident energy at the indicated scattering angles. Note how the spectrum changes with scattering angle as a result of varying contributions of different electronics states.

of electronic states are known[7, 19, 20] to produce large anomalies in the vibrational spacings and associated Franck-Condon factors in many of the vibrational levels of electronic states in this energy-loss region. Vibrational energy levels for the b', c, and c' states were taken from Dressler,[19] those for the b state from Carroll and Collins,[20] those for the o state from Geiger and Schröder,[7] and those for the remaining states from Joyez *et al.*[14] Franck-Condon factors for the singlet states were determined by combining relative intensity results[7] with the unity sum rule for Franck-Condon factors. Those for the triplet states were determined in the same manner as the singlet states, but from data of Joyez *et al.*[14] Since the two unknown states, $M1$ and $M2$, make nearly identical contributions in the spectra of Joyez *et al.*,[14] it was assumed, for lack of information to the contrary, that the excitation cross sections for those two states were essentially identical.

The least-squares best fit of the energy-loss spectrum yields the DCS, *relative* to the elastic scattering, for excitation of each electronic transition at the given angle and incident electron energy. Multiplication of this inelastic-to-elastic intensity ratio by the absolute elastic scattering DCS at the appropriate energy and scattering angles places the inelastic spectrum on the absolute cross-section scale. The latter elastic DCS's were taken from recent measurements in this labatory.[21]

An energy-level diagram showing the location of vibrational levels in each electronic state included in the spectral decomposition is shown in Fig. 1. Because of strong perturbations among the singlet states, the usual potential energy curves could not be drawn for these states. In Fig. 2 are shown raw energy-loss spectra at 40 eV incident energy and at several scattering angles in order to illustrate the varying contributions of the different electronic transitions as a function of scattering angle. An example of the spectral decomposition is shown in Fig. 3.

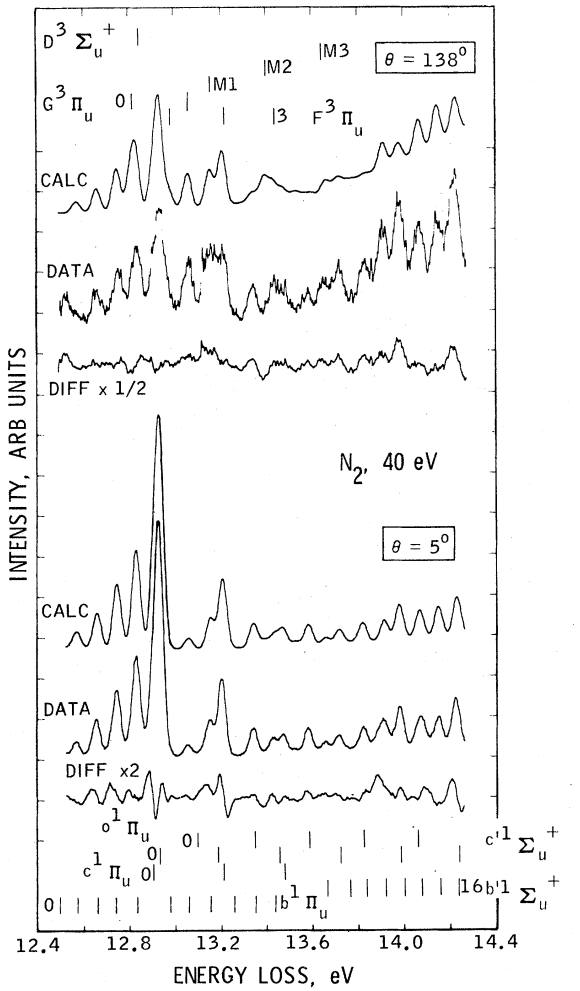

FIG. 3. Electron-impact energy-loss spectra of N_2 at the indicated energy and angles. At each angle are given the raw ("DATA"), computer-generated ("CALC") and difference ("DIFF") spectra. Note the scale changes on the different spectra. Also given are energy locations of all singlet and triplet excitations used in the data unfolding to obtain the "CALC" spectrum. Unidentified triplet transitions $M1$, $M2$, and $M3$ are also indicated. The location and intensity of these excitations were dictated by requirements of a best least-squares fit between the raw and theoretical spectra.

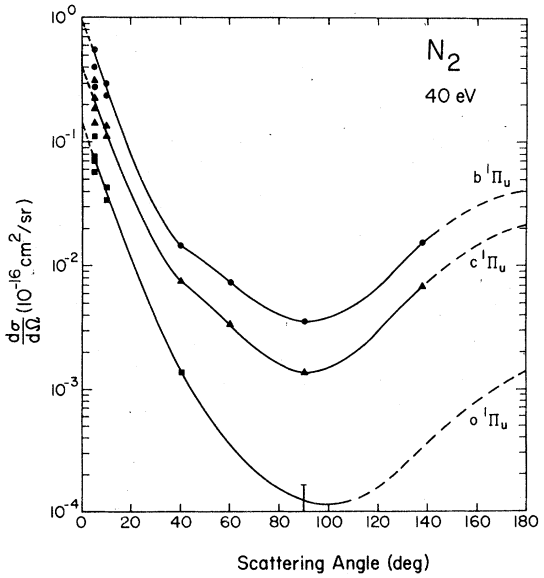

FIG. 4. Absolute differential cross sections for excitation to the b, c and o states of N_2 at 40 eV incident energy. Dashed lines denote extrapolations to 0° and 180° scattering angles.

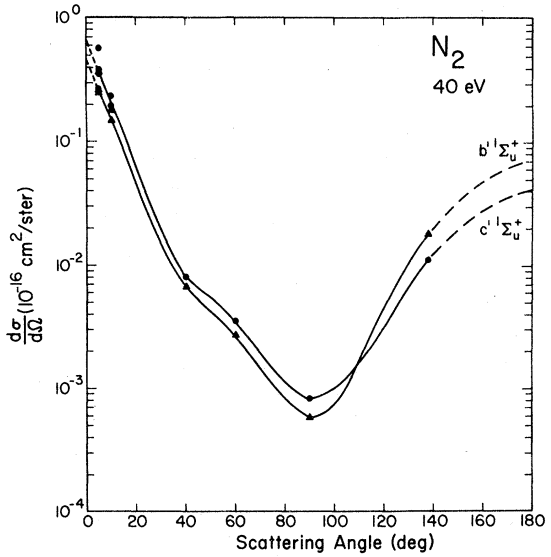

FIG. 5. Same as Fig. 4, but for the b' and c' states of N_2.

III. RESULTS

Differential cross sections at 40 eV incident energy for excitation from the ground $X\,^1\Sigma_g^+$ state to the three $^1\Pi_u$ states ($b, c,$ and o) are shown in Fig. 4; for excitation to the two $^1\Sigma_u^+$ states (b' and c') in Fig. 5; and those for excitation to the $^3\Pi_u$ states (F and G) and to the two unknown states ($M1$ and $M2$) shown in Fig. 6. DCS's for excitation of these same states at 60 eV incident energy are given in Fig. 7 ($^1\Pi_u$ states), Fig. 8 ($^1\Sigma_u^+$) states, and Fig. 9 ($^3\Pi_u$ and unknown states).

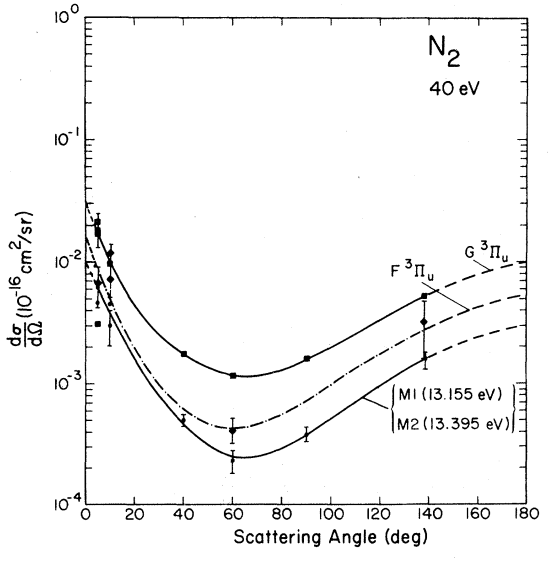

FIG. 6. Same as Fig. 4, but for the G, F, and unidentified triplet states $M1$ and $M2$. Shown are the results for $M1$ or $M2$, the two contributions being taken as equal in the data analysis.

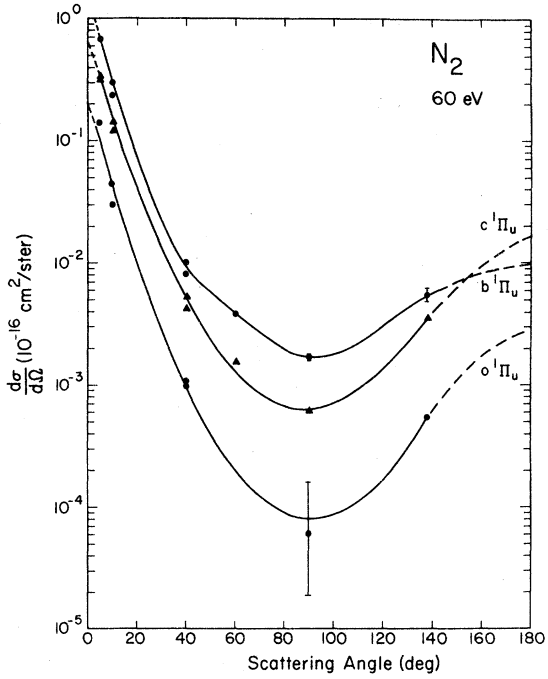

FIG. 7. Same as Fig. 4, but at 60 eV incident electron energy.

Integral cross sections for excitation of these eight electronic states are shown in Figs. 10 and 11. Solid curves in these figures were drawn to pass through the two measured values at 40 and 60 eV, and through the zero value at the threshold for each state. As a result of the few data points

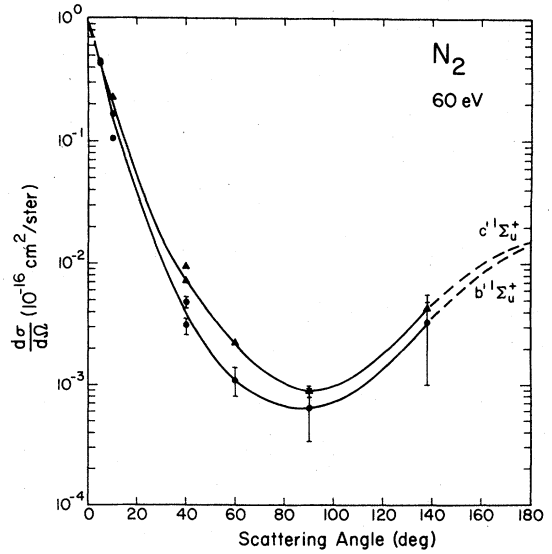

FIG. 8. Same as Fig. 5, but at 60 eV incident electron energy.

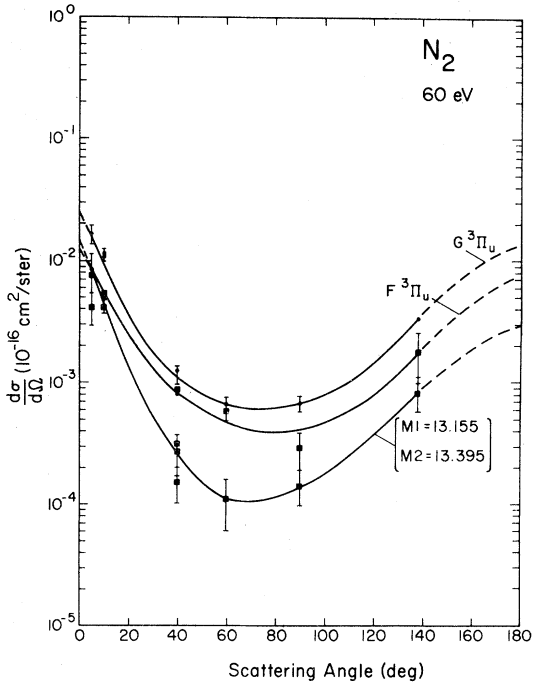

FIG. 9. Same as Fig. 6, but at 60 eV incident electron energy.

through which these curves have been drawn, these integral cross sections are not as accurately known as those for the valence states (paper II). Tabulated values of all integral and differential cross sections are presented in Tables I and II at 40 and 60 eV, respectively. There are no other measurements to which the present results can be compared.

The statistical error present in each data point as a result of the spectral decomposition is indicated by an error bar, unless that error is smaller than the plotted symbol. A fuller discussion of these types of errors is given in Sec. III E of paper I.

From the DCS's in Tables I and II one may derive a generalized oscillator strength $f_{GOS}(K)$, as a function of momentum transfer K, for each electronic state. One may then see from the present measurements how closely $f_{GOS}(K)$ approaches the optical f value in the limit as K^2 approaches zero.

For a discrete transition, the generalized oscillator strength is defined by

$$f_{GOS}(K) = 0.5\ (k/k')K^2 \Delta E (d\sigma/d\Omega)\ , \qquad (1)$$

where k and k' are the initial and final electron momenta, respectively; K^2 the square of the momentum transfer to the target, ΔE the energy loss, and $d\sigma/d\Omega$ the DCS. All quantities are in atomic units (k, k' in a_0^{-1}; $d\sigma/d\Omega$ in $a_0^2\,\mathrm{sr}^{-1}$; $K^2, \Delta E$ in Hartree). Results for $f_{GOS}(K)$ plotted against K^2 for the five optically

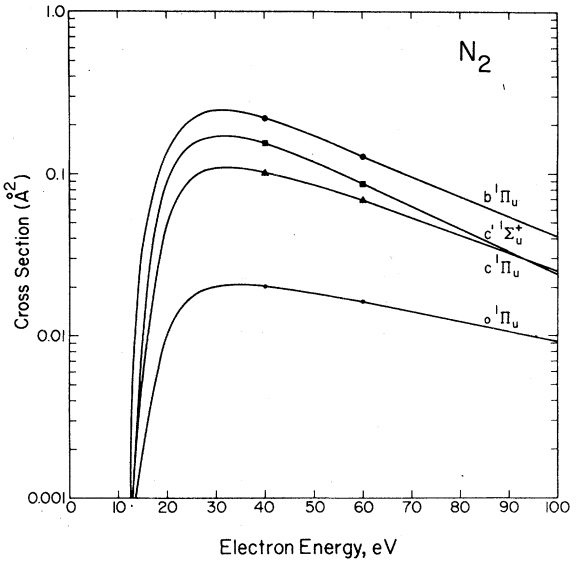

FIG. 10. Integral cross sections for the b, c, o, and c' states of N_2. Solid curves for each state have been artistically drawn to rise from the respective thresholds and pass through the 40 and 60 eV measured points.

allowed transitions are shown in Figs. 12 and 13. Error bars in these calculated values are those of $d\sigma/d\Omega$, and are usually about ± 20%. Also plotted in Fig. 12 for the $b\ ^1\Pi_u$ state are absolute absorption f values derived from the 3-0 and 4-0 bands of the $b \leftarrow X$ transition. These values were obtained by dividing the individual band f values of Lawrence *et al.*[15] (their Table I) by the appropriate Franck-Condon factor to obtain the f values for the entire electronic transition.

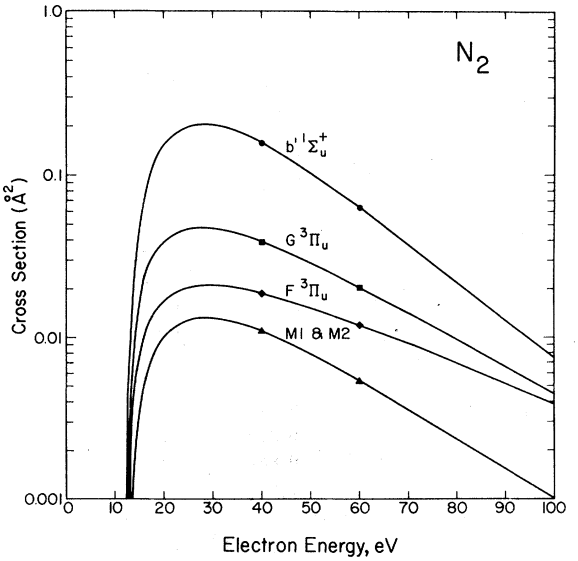

FIG. 11. Same as Fig. 10, but for the b', G, F and one of the $M1$ or $M2$ states.

TABLE I. Differential and integral cross sections for singlet and triplet electronic states of N_2 at E_0 of 40 eV. All units are 10^{-16} cm^2/sr.

θ (deg) [a]	Elastic [b]	$b\,^1\Pi_u$ (10^{-2})	$c\,^1\Pi_u$ (10^{-2})	$o\,^1\Pi_u$ (10^{-3})	$b'\,^1\Sigma_u^+$ (10^{-2})	$c'\,\Sigma_u^+$ (10^{-2})	$G\,^3\Pi_u$ (10^{-2})	$F\,^3\Pi_u$ (10^{-2})	$M1(-M2)$ [c] (10^{-3})
(0)	11.1	92.0	40.0	140	46.0	66.0	3.10	1.63	10.0
(10)	6.70	25.5	11.2	39.0	14.8	21.0	1.00	0.500	3.80
20	3.50	7.50	3.70	11.5	4.60	6.10	0.440	0.190	1.58
30	1.85	2.80	1.42	3.70	1.50	1.91	0.255	0.098	0.78
40	0.83	1.44	0.750	1.40	0.670	0.800	0.175	0.061	0.46
50	0.44	1.05	0.510	0.66	0.420	0.540	0.135	0.047	0.31
60	0.26	0.740	0.340	0.35	0.270	0.350	0.117	0.045	0.25
70	0.16	0.520	0.215	0.22	0.142	0.190	0.117	0.047	0.25
80	0.11	0.410	0.160	0.15	0.083	0.112	0.131	0.056	0.29
90	0.09	0.355	0.138	0.12	0.058	0.082	0.161	0.073	0.38
100	0.09	0.385	0.150	0.12	0.074	0.098	0.200	0.098	0.52
110	0.15	0.480	0.200	0.13	0.172	0.161	0.260	0.133	0.71
120	0.29	0.680	0.300	0.16	0.450	0.310	0.335	0.177	0.96
130	0.52	1.09	0.480	0.24	1.04	0.670	0.433	0.230	1.30
(140)	0.88	1.67	0.750	0.37	2.00	1.22	0.550	0.290	1.65
(150)	1.32	2.34	1.10	0.56	3.25	1.95	0.670	0.360	2.05
(160)	1.83	3.10	1.50	0.80	4.70	2.75	0.800	0.425	2.45
(170)	2.29	3.70	1.87	1.10	6.00	3.50	0.920	0.490	2.80
(180)	2.55	4.20	2.15	1.40	7.00	4.00	1.00	0.540	3.00
Integral	9.16	21.8	10.0	20.0	15.6	15.3	3.90	1.90	11.0

[a] Values of cross sections at angles given in parentheses are obtained by extrapolation of the elastic DCS's.
[b] From Ref. 21. The slightly different integral elastic cross section in the present work arises from a different extrapolation of the elastic DCS to higher and lower angles.
[c] The cross sections for excitation of states $M1$ and $M2$ appear to be the same based on Joyez *et al.* (Ref. 14) and the present work.

TABLE II. Differential and integral cross sections for singlet and triplet electronic states of N_2 at E_0 of 60 eV. All units are 10^{-16} cm^2/sr.

θ (deg) [a]	Elastic [b]	$b\,^1\Pi_u$ (10^{-2})	$c\,^1\Pi_u$ (10^{-2})	$o\,^1\Pi_u$ (10^{-3})	$b'\,^1\Sigma_u^+$ (10^{-2})	$c'\,^1\Sigma_u^+$ (10^{-2})	$G\,^3\Pi_u$ (10^{-2})	$F\,^3\Pi_u$ (10^{-2})	$M1(=M2)$ [c] (10^{-3})
(0)	10.9	130	64	200	90.0	85.0	2.40	1.30	14.0
(10)	6.20	30.0	15	44.0	15.0	20.0	0.920	0.540	4.30
20	3.15	7.40	4.30	10.0	3.50	5.00	0.350	0.245	1.35
30	1.40	2.25	1.31	2.80	1.00	1.60	0.175	0.132	0.52
40	0.60	0.920	0.510	1.00	0.380	0.710	0.111	0.084	0.26
50	0.29	0.570	0.230	0.39	0.180	0.370	0.082	0.060	0.15
60	0.18	0.390	0.130	0.20	0.110	0.220	0.067	0.047	0.11
70	0.11	0.265	0.085	0.12	0.079	0.140	0.062	0.041	0.10
80	0.09	0.197	0.067	0.09	0.067	0.103	0.063	0.040	0.11
90	0.08	0.170	0.052	0.08	0.064	0.090	0.068	0.042	0.14
100	0.10	0.180	0.071	0.09	0.073	0.098	0.080	0.048	0.18
110	0.18	0.220	0.094	0.11	0.094	0.127	0.103	0.060	0.25
120	0.30	0.310	0.136	0.17	0.134	0.184	0.144	0.080	0.37
130	0.42	0.435	0.225	0.30	0.210	0.290	0.225	0.120	0.58
(140)	0.54	0.570	0.400	0.61	0.360	0.460	0.375	0.200	0.90
(150)	0.64	0.710	0.650	1.10	0.560	0.700	0.590	0.310	1.36
(160)	0.72	0.840	0.960	1.70	0.830	0.990	0.850	0.460	1.90
(170)	0.74	0.940	1.33	2.35	1.13	1.28	1.12	0.620	2.50
(180)	0.72	0.980	1.62	2.80	1.41	1.50	1.40	0.780	3.00
Integral	6.61	12.7	6.90	16.0	6.30	8.80	2.00	1.20	5.30

[a] Values of cross sections at angles given in parentheses are obtained by extrapolation of the elastic DCS's.
[b] From Ref. 21.
[c] The cross sections for excitation of states $M1$ and $M2$ appear to be the same based on Joyez *et al.* (Ref. 14) and the present work.

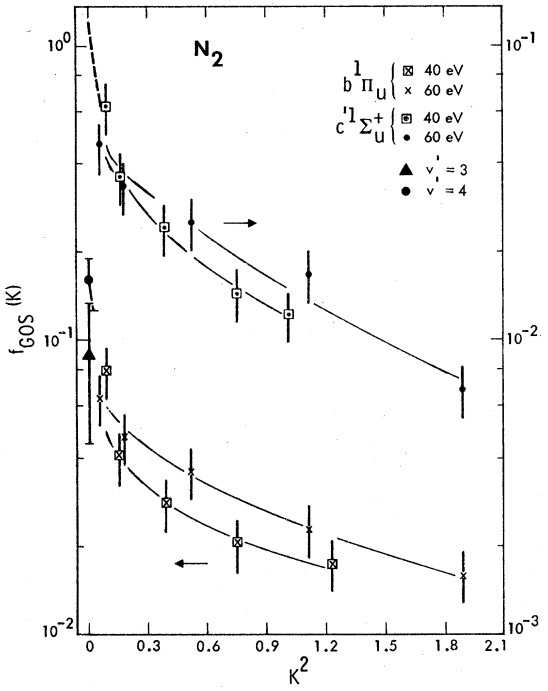

FIG. 12. Generalized oscillator strength plotted vs the square of the momentum transfer for the $b\,^1\Pi_u$ and $c'\,^1\Sigma_u^+$ states. Points denoted as $v'=3$ and $v'=4$ at zero momentum transfer are derived from optical oscillator-strength measurements of Ref. 15 for the b state. The smallest value of K^2 in the present measurements corresponds to a scattering angle of 5°. Dashed line for the c' state shows the extrapolation to zero momentum transfer from which the optical f value for the c' state was obtained.

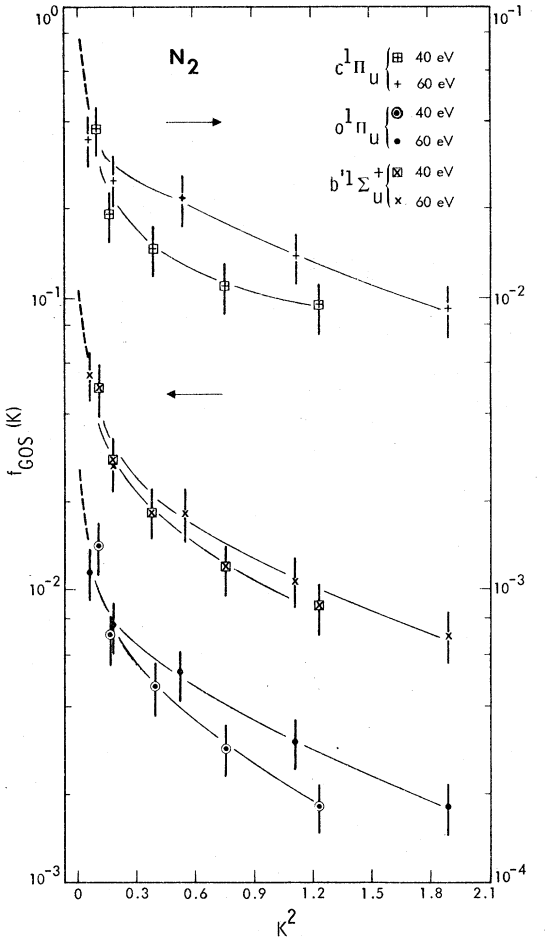

FIG. 13. Same as Fig. 12, but for the c, o, and b' states.

IV. DISCUSSION

A. Spectroscopic considerations

While assignments within the optically allowed states are fairly unambiguous, assignments of the triplet excitations included in the unfolding were subject to more uncertainty. The spectral decomposition procedure, which can serve as a cross check of the assignments, was able to accommodate the F, G, $M1$, and $M2$ states in the deconvolution. However, no consistent contribution of the D and $M3$ states could be found, either because these states were only weakly present, or their energy locations were not optimally adjusted within experimental errors. Thus, cross sections for these states could not be determined. They are the only singlet or triplet states within 14.2 eV of the ground state for which a cross section was not obtained in this study (papers I, II, and III in this series).

From earlier electron-impact observations of the same energy-loss region an unidentified state at 13.2 eV (actually at 13.18 eV) was observed (see Ref. 12, Fig. 6). This state appeared to have triplet angular behavior and was thus distinct from the nearby 1-0 ($c'\,^1\Sigma_u^+$) and 1-0 ($c\,^1\Pi_u$) optically allowed bands. In the present work state $M1$ at 13.155 ± 0.01 eV appears to correspond in energy (within experimental error) and spin character to the unidentified triplet state of Ref. 12.

B. Differential and integral cross sections

The DCS's of Figs. 4, 5, 7, and 8 for the optically allowed transitions show a similar behavior to one another. The DCS's are characteristically strongly forward-peaked, corresponding to the long-range dipole interaction experienced in the scattering process. This forward peaking is greater at 60 eV than at 40 eV, and the DCS's for excitation of these dipole states rise in the backward direction to a value roughly one-tenth the forward cross sections. All DCS's exhibit a minimum near 90° scattering angle.

The DCS's for excitation of the triplet states (Figs. 6 and 9) are less forward-peaked than those of the singlets, and appear to rise at large scattering angles to a cross section comparable to the low-angle value. This behavior is consistent with the shorter-range nature of the electron exchange forces. That is, particle exchange requires close collisions which correspond to large angles of scattering. It is also noted that the DCS for excitation of the triplet states have minima near 70° scattering angle.

Integral cross sections for all the states (Figs. 10 and 11) are smaller at the higher impact energy (60 eV) so that the peaks of the integral cross sections probably lie at or below 40 eV. Since some artistic license was used in drawing the smooth curves shown in these figures, the precise value is not accurately known. Comparison of these integral cross sections with those in paper II reveals that the former are generally smaller than those of the valence states, with only the b, c', and b' cross sections reaching values larger than 0.1 Å^2.

C. Generalized oscillator strengths

Two points become clear from Figs. 12 and 13. First, results for $f_{GOS}(K)$ calculated from the 40 eV data generally lie below results from the 60 eV data. It is thus apparent that these impact energies are not sufficient to attain the Born limit where $f_{GOS}(K)$ becomes independent of the incident electron energy. Secondly, one sees that $f_{GOS}(K)$ for the $b \leftarrow X$ transition (Fig. 12) at smaller values of K^2 is rising to meet the optical f value results.[15] However, an extrapolation to zero momentum transfer from data of this study is still quite uncertain as $f_{GOS}(K)$ at the smallest K^2 is yet approximately one-half the optical f value. Another comparison is possible based on the summed $f_{GOS}(K)$ [denoted here as $f^S_{GOS}(K)$] over the energy-loss range 11.4–13.6 eV. A value of[11,22] 0.66 ± 0.07 has been previously reported for $f^S_{GOS}(K)$.

TABLE III. Extrapolated optical f values for excitation of the b, c, o, b', and c' states from data of Figs. 12 and 13.

Transition	Optical f value Present extrapolation [a]	Ref. 15
$b\ ^1\Pi_u \leftarrow X$	···	0.16 [b]
$c\ ^1\Pi_u \leftarrow X$	0.080	
$o\ ^1\Pi_u \leftarrow X$	0.026	
$b'\ ^1\Sigma_u^+ \leftarrow X$	0.10	
$c'\ ^1\Sigma_u^+ \leftarrow X$	0.12	

[a] ± 50%.
[b] From 4-0 band measurement.

An independent value of 0.40 has also been estimated for the same energy-loss interval.[9,15] The sum $f^S_{GOS}(K)$ in the present work for all the transitions in the 12.5–14.2 eV interval gives a value of only 0.33. While part of this difference undoubtedly arises from the slightly different energy-loss intervals in the summation, we believe a major part is due to the extrapolation error discussed above and shown in Fig. 12.

Results such as those shown in Figs. 12 and 13 indicate that care must be taken in extrapolating any GOS to an optical f value at these relatively low electron energies. However, with the obvious shortcomings as evident in Figs. 12 and 13 in mind, one may obtain a crude optical f value by extrapolating to $K^2 = 0$ for the remaining four optical transitions shown in these figures. This extrapolation was carried out by using an identical shape into the $K^2 = 0$ limit as that required in Fig. 12 to go to the $v' = 4$, $b \leftarrow X$ optical f value. Results of this extrapolation are presented in Table III, along with the one other experimental value. The accuracy of the extrapolated f value is probably no better than ±50%. These values are meant to provide an estimate where none presently exists.

‡Work supported by the National Aeronautics and Space Administration under Contract NAS7-100 to the Jet Propulsion Laboratory, and by the U. S. Energy Research and Development Administration under Contract W-7405-ENG 36 to Los Alamos Scientific Laboratory.

[1]W. R. Bennett, Appl. Optics Supp. on Chemical Lasers (1965); G. G. Petrash, Sov. Phys. Usp. 14, 747 (1972); C. K. Rhodes, IEEE J. Quant. Electron. QE-10, 153 (1974).
[2]A. Vallance-Jones, Aurora, Geophysics and Astrophysics Monographs, Vol. 9 (1974).
[3]M. B. McElroy, T. Y. Kong, Y. L. Yung, and A. O. Nier, Science 194, 1295 (1976).
[4]D. C. Cartwright, A. Chutjian, S. Trajmar, and W. Williams, Phys. Rev. A 16, 1013 (1977), paper I, this issue.
[5]D. C. Cartwright, S. Trajmar, A. Chutjian, and W. Williams, Phys. Rev. A 16, 1041 (1977), paper II, this issue.
[6]J. Geiger and W. Stickel, J. Chem. Phys. 43, 4535 (1965).
[7]J. Geiger and B. Schröder, J. Chem. Phys. 50, 7 (1969).
[8]E. N. Lassettre, A. Skerbele, M. A. Dillon, and K. J.

Ross, J. Chem. Phys. 48, 5066 (1968).
[9]E. N. Lassettre, Can. J. Chem. 47, 1733 (1969).
[10]V. D. Meyer, A. Skerbele, and E. N. Lassettre, J. Chem. Phys. 43, 3769 (1965).
[11]S. M. Silverman and E. N. Lassettre, J. Chem. Phys. 42, 3420 (1965).
[12]A. J. Williams, III and J. P. Doering, J. Chem. Phys. 51, 2859 (1969).
[13]A. J. Williams, III and J. P. Doering, Planet. Space Sci. 17, 1527 (1969).
[14]G. Joyez, R. I. Hall, J. Reinhardt, and J. Mazeau, J. Electron. Spectrosc. Rel. Phenom. 2, 183 (1973).
[15]G. M. Lawrence, D. L. Mickey, and K. Dressler, J. Chem. Phys. 48, 1989 (1968).
[16]A. Chutjian, D. C. Cartwright, and S. Trajmar, Phys. Rev. Lett. 30, 195 (1973).
[17]S. Trajmar, D. C. Cartwright, and W. Williams, Phys. Rev. A 4, 1482 (1971).
[18]A. Chutjian, J. Chem. Phys. 61, 4279 (1974).
[19]K. Dressler, Can. J. Phys. 47, 547 (1969).
[20]P. K. Carroll and C. P. Collins, Can. J. Phys. 47, 563 (1969).
[21]S. K. Srivastava, A. Chutjian, and S. Trajmar, J. Chem. Phys. 64, 1340 (1976).
[22]E. N. Lassettre, private communication.